THE JOURNAL OF PHYSICAL CHEMISTRY C

Article

pubs.acs.org/JPCC

Coupling of Cobalt–Tetraphenylporphyrin Molecules to a Copper Nitride Layer

Vinícius Claudio Zoldan,[†,‡] Ricardo Faccio,[§] Chunlei Gao,[†] and André Avelino Pasa*[,‡]

[†]Max Planck Institute of Microstructure Physics, Halle, Germany

[‡]Laboratório de Filmes Finos e Superfícies, Universidade Federal de Santa Catarina, Brazil

[§]Cryssmat-Lab and Centro NanoMat, Facultad de Química, Universidad de la República, Montevideo, Uruguay

ABSTRACT: For applications such as molecular electronics and spintronics, it is very important to accurately describe the interface between molecular species and the underlying surfaces. In this work, we have used low temperature scanning tunneling microscopy to study the physical and chemical interaction between individual cobalt–tetraphenylporphyrin molecules and a copper nitride monolayer. We have demonstrated that the Cu_3N–Cu(110) system promotes a selective decoupling of the porphyrin macrocycle from the local environment, allowing visualization of the molecular orbitals and vibronic states of the molecule, while maintaining a strong coupling between the Co-d_{z^2} orbital and the substrate. The reverse behavior was observed for adsorption of the same molecule onto a metallic Cu(110) surface. First-principles calculations confirm both the molecular adsorption site and the electronic decoupling of the molecular states from the substrate.

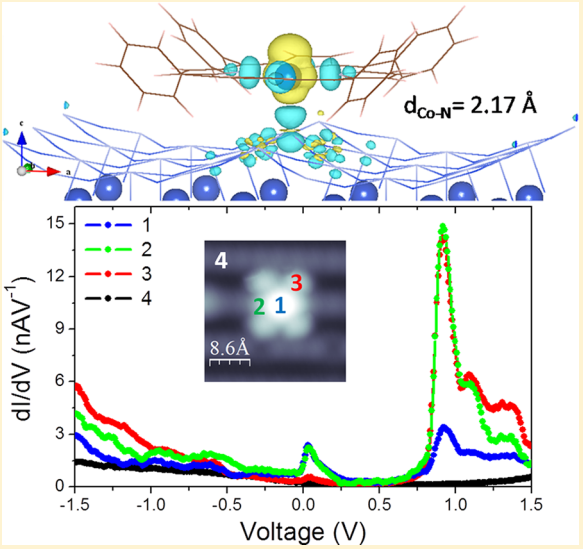

INTRODUCTION

The electronic and magnetic coupling between molecules and surfaces is of general interest for molecular electronics, molecular magnets, spintronics, and quantum computing. Additionally, the preparation and manipulation of low-dimensional systems is of fundamental importance to solid-state physics. In this context, one family of molecules that has attracted great attention are porphyrins,[1−6] which can host a large variety of metal atoms[7,8] and have been studied as single molecules, self-assembled thin films, and bulk materials.

The electronic and magnetic properties of metal–organic complexes are strongly affected by the density of states of the substrate to which they are adsorbed.[9−14] The coupling between the molecule and the substrate causes energy shifts and mixture and broadening of discrete molecular orbitals.[15] Therefore, in an effort to obtain a detailed understanding of the intrinsic properties of the molecule and its potential use in applications such as molecular electronics, it is important to investigate systems where electronic decoupling between the molecule and the substrate is observed. Ultrathin insulating layers have been used to control the surface electron density and consequently the coupling of molecules to the substrate.[12] This approach allows the direct imaging of molecular orbitals similar to the ones observed for free molecules. The insulating spacer layer also increases the lifetime of transient molecular charge states, allowing the detection of vibronic states via STM conductance measurements.[16]

In this work, we use a low-temperature scanning tunneling microscope (LT-STM) to demonstrate that a monolayer of Cu_3N can be used to reduce the interaction between a Co–TPP (cobalt–tetraphenylporphyrin) molecule and the Cu(110) substrate, allowing the observation of both vibronic states and the corresponding density of states of the C atoms similar to that observed for the molecule in the gas phase. First-principles calculations based on density functional theory (DFT)[17−19] were carried out to obtain the structural configuration and the electronic properties of the Co–TPP molecule on both Cu(110) and Cu_3N–Cu(110) substrates.

The Co–TPP/Cu_3N–Cu(110) system is unique because the porphyrin macrocycle experiences little interaction with the substrate despite the fact that the central Co atom is strongly anchored to the surface with strong coupling with the N atom, majorly due to a Co-d_{z^2}/N-p_z interaction. In addition, another surprising result is the capacity of the Cu_3N monolayer to allow single molecule room temperature deposition and stability, what is of significant importance for future device fabrication.

Received: February 6, 2013
Revised: July 10, 2013
Published: July 11, 2013

The DFT results support the role of the Cu_3N as a selective decoupling monolayer. According to calculations, Co−TPP molecule is decoupled in terms of interactions between states from the porphyrin macrocycle, but at the same time the Co atom is strongly coupled in terms of the interaction of Co-d_{z^2}/N-p_z states, giving place to a selective or differential decoupling between Co−TPP molecule and Cu_3N−Cu(110) surface. For these reasons, we denominate this behavior as a selective hybridization, which is fundamental for the understanding of the electronic structure of the system.

EXPERIMENTAL AND THEORETICAL METHODS

Experimental Section. The experiments were carried out in a low-temperature STM system operated at 4.6 K, consisting of three separate ultrahigh vacuum (UHV) chambers used for substrate preparation, molecular deposition, and STM measurements. The single crystal Cu(110) sample was cleaned by repeated cycles of 2000 eV Ar^+ ion sputtering and annealing at 750 K. The copper nitride Cu_3N surface was prepared on a clean Cu(110) substrate following the recipe presented in ref 20. N_2 was introduced into the chamber at a constant pressure of 1.1×10^{-8} mbar and activated by bombarding through an ion gun with beam energy of 450 eV, while the sample was kept at 690 K. Low energy electron diffraction measurements displayed a p(2 × 3) pattern (results not shown) characteristic of copper nitride as expected.[20] The copper nitride thin film covers the entire copper substrate, and the surface is composed of atomically flat terraces with typical widths on the order of hundreds of nanometers. Figure 1a shows a high-resolution STM image of the Cu_3N layer, where the distance along the $(1\bar{1}0)$ and (001) directions of the (2 × 3)N unit cell are 5 and 11 Å, respectively. The Co−TPP (cobalt−tetraphenylporphyrin) molecules were purified by vacuum sublimation prior to deposition on the Cu(110) and Cu_3N−Cu(110) surfaces. During the deposition, the substrates were kept at room temperature. Spectroscopic measurements were performed using the lock-in amplifier technique with a 5 mV sine wave applied to the sample bias. Images obtained at positive/negative sample bias voltage corresponds to unoccupied/occupied states, and 0 V represents the position of the Fermi level. All spectra taken of the molecules were compared with the dI/dV spectra of the clean substrate both before and after measuring the molecule to avoid tip effects.

Computational Methods. The theoretical study is based on first-principles density functional theory[17,18] and the model used for the system Co−TPP/Cu_3N−Cu(110) consists of a single Co−TPP molecule situated above the Cu_3N monolayer, which itself was constructed on a 5 layer Cu(110) slab. The simulations were performed using the ab initio program VASP (Vienna ab initio simulation program)[21−24] developed at the Institut für Material Physik of the Universität Wien. The PBE[25] generalized gradient approximation (GGA) functional has been used, and the projector-augmented wave method (PAW)[26,27] has been employed to treat the atomic cores. The precision setting for the VASP calculations was set to the one that corresponds to a global plane-wave energy cutoff of 500 eV. The size of the grid was 120 × 90 × 144 points per k-point, and a grid of 4 × 4 × 1 k-point has been used.

The vibrational spectra was determined utilizing Gaussian09[28] using hybrid exchange correlation functional B3LYP with the 6-311G* basis set.

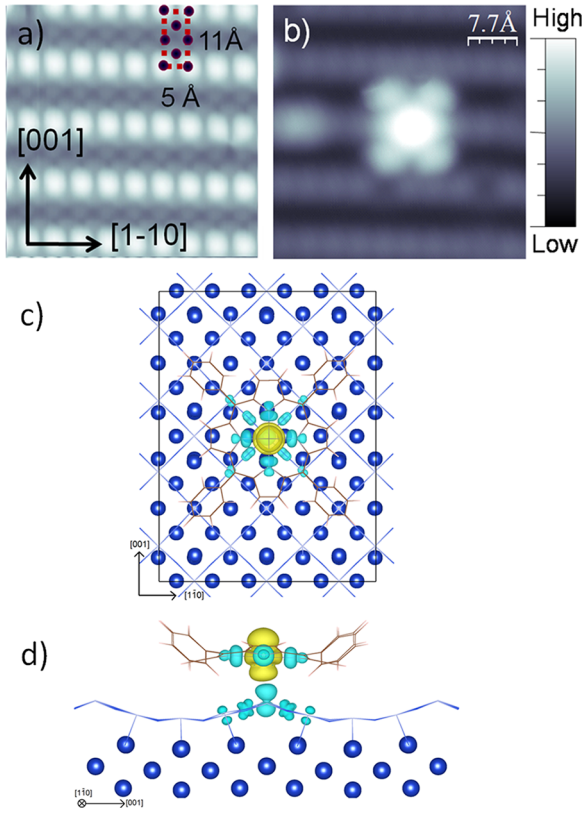

Figure 1. (a) High-resolution STM image of the Cu_3N monolayer. A schematic shows the placement of the N atoms of the (2 × 3)N reconstruction (blue circles). The lattice is based on the structural model of ref 20. (b) STM image of a Co−TPP molecule adsorbed on the ordered copper nitride/Cu(110), recorded at V = −1.0 V and I = 0.5 nA. Top view (c) and lateral projection (d) of the structural model for Co−TPP molecule deposited on the Cu_3N surface. The simulated spin density map for the optimized relaxed structure showing the half-filled Co-d_{z^2} orbital is also presented. The light blue and yellow colors represent the up and down spins, respectively.

RESULTS AND DISCUSSION

Co−TPP on Cu_3N−Cu(110). Figure 1a displays a typical STM image of the Cu_3N−Cu(110) surface, which is terminated by rows of N atoms. Co−TPP was deposited onto this surface at submonolayer coverage in an effort to study individual molecules. Figure 1b shows an STM image of a single Co−TPP molecule on top of this surface. The molecule can be described as a protrusion with a central bright feature, due to the cobalt atom in the center of porphyrin macrocycle, and four legs, corresponding to the phenyl rings. Through analysis of several individual molecules, we conclude that the center of the TPP molecule is located above the rows of nitrogen atoms with the four legs (phenyl groups) positioned in the Cu_3N troughs, that is, the molecule assemblies centered on the bright spots over the substrate rows, orientated in the $(1\bar{1}0)$ direction, as can be seen in the figure.

Figure 1c shows a top view structural model of the planar Co−TPP molecule as it sits above the highest N rows of the (2 × 3)N reconstruction. A full ionic optimization, with a fixed unit cell, of the molecule on the Cu_3N monolayer confirms the experimental observation that the Co atom is sitting on the top of the N row, and specifically atop an N atom. Figure 1d shows that the optimized structure has a very short cobalt to nitrogen distance of d_{Co-N} = 2.72 Å. Additionally, the strong STM signal

dx.doi.org/10.1021/jp4013625 | J. Phys. Chem. C 2013, 117, 15984−15990

at the center of the porphyrin molecule in Figure 1b is in agreement with the simulation, which shows the Co in a low spin state ($S = 1/2$) with a half-filled d_{z^2} orbital.

Figure 2a shows the dI/dV spectra taken at different positions above the Co−TPP molecule, as indicated in the inset STM image. For the voltage range −1.5 to +1.5 V, two peaks are observed at the center of the molecule (position 1), one close to the Fermi level and another at 0.92 eV corresponding to LUMO/LUMO+1 states. For energies less than −0.5 eV, a noticeable increase of the signal was observed in the dI/dV spectra, but these broad, low intensity features do not correspond to what would be expected for HOMO peaks. The peak at the Fermi level could be attributed to a Kondo effect, as previously reported for both Fe− and Co−phthalocyanine molecules after the decoupling from the underlying substrate.[10,29] However, the direct observation of this effect by STS measurements is complex due to localized ionized states and their crystal field splitting.[30] At positions 2 and 3, the STM tip probes the pyrrolic ring and the methine bridge (region connected to the phenyl ring) of the porphyrin macrocycle, respectively. The contribution of the LUMO/LUMO+1 is stronger and sharper at these locations, suggesting the decoupling of the porphyrin ring from the surface. This effect could also be explained by the local molecular orbitals; however, when comparing the same molecule on others substrates, we observed that the peaks are more strong and sharp on copper nitride surfaces (see Figure 4a for Co−TPP on Cu(110)). In order to check if the induced electric field from the STM tip influences the position of the LUMO/LUMO+1 states for this system,[31] we measured the position of these peaks at different tip/molecule distances, and no significant deviation from the original position at 0.92 V was observed.

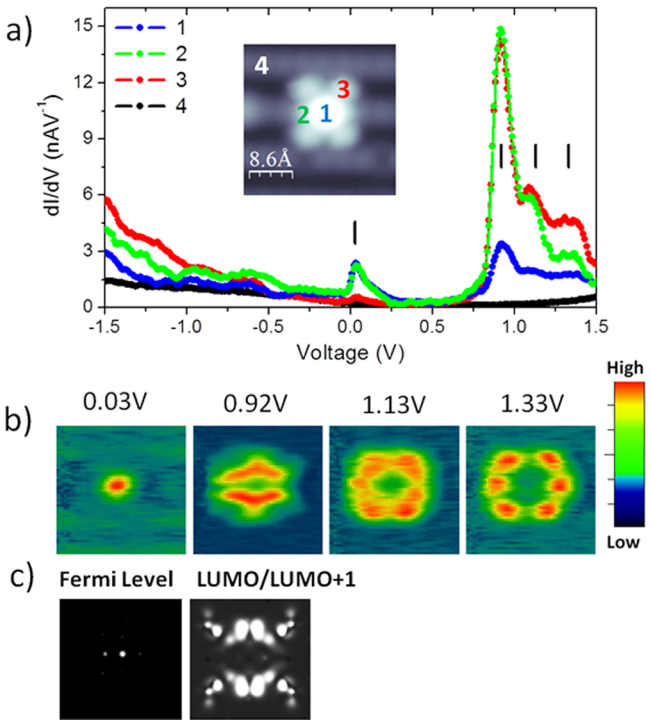

Figure 2. (a) dI/dV spectroscopy at three different positions above a single Co−TPP molecule as indicated in the inset STM image recorded at 0.96 V bias and 0.62 nA tunneling current. The spectra were taken with an open feedback loop at initial parameters of I = 1.0 nA and V = −1.0 V. The dI/dV signal for the substrate is also shown for reference. (b) dI/dV maps at different voltages and (c) simulated STM obtained at Fermi level and LUMO/LUMO+1 positions. Note: in the case of simulated STM map at Fermi level some contribution from N atoms appears as small dots around the central spot.

For positions 2 and 3, two additional peaks are clearly observed for voltages higher than 1.0 V. These peaks, which are also present at position 1 but with lower intensity, are attributed to vibronic states of the molecule.[9] The curve corresponding to position 4 was added to show that the copper nitride monolayer has a reduced conductance compared to the molecular conductance and does not contribute with peaks in the energy range of interest.

Figure 2b shows the dI/dV maps at four different voltages, 0.03, 0.92, 1.13, and 1.33 V, and Figure 2c presents the corresponding theoretical STM simulations for 0.03 and 0.92 V, as obtained by using the Tersoff−Hamann method[32] with a constant height of 3 Å above the topmost H atoms of the CoTPP. Some dissimilarities between experiment and simu-

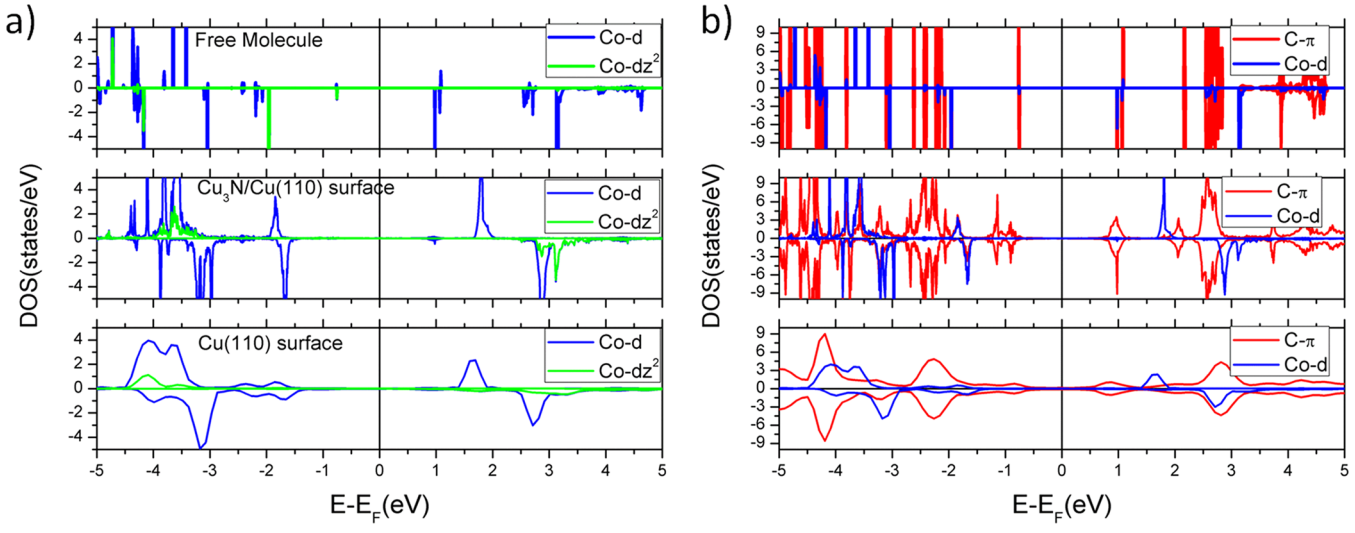

Figure 3. Density of states as calculated for the molecule in the gas phase, absorbed on Cu_3N−Cu(110) and absorbed on Cu(110), for Co-d and Co-d_{z^2} states (a) and Co-d and Co-π states (b).

dx.doi.org/10.1021/jp4013625 | J. Phys. Chem. C 2013, 117, 15984−15990

lation could be arisen from the tip in theoretical model, that considers a single atom at the apex,[33] the short distance between tip and molecule, and the xc-potential utilized in the calculations, which may slightly modify the structural geometry. For example, van der Waals corrected xc-potential[34−36] could enhance the C-π and surface interactions, in comparison to our selected GGA-PBE xc-potential with some small differences in the final geometries.

The dI/dV map at 0.03 V shows the contribution of Co close to the Fermi level. This simulated map, Figure 2c, display also the contribution from N atoms as small dots around the central spot. The dI/dV map obtained at 0.92 V corresponds to the LUMO and LUMO+1 states of the molecule, as can be inferred from ab initio calculations reported by others[31] and confirmed by us as well. At this potential, no feature is observed in the center of the molecule, corresponding to contributions of the Co atom, as confirmed by the spectra simulation for the Co-d levels after the absorption on the Cu_3N monolayer, as will be discussed in Figure 3. The CoTPP LUMO/LUMO+1 molecular orbital presents two orthogonal nodal planes that intersect at the Co position. Because of the interaction of Co−TPP with the surface, a deformation occurs where two pyrrole C−H bonds come upward and the remaining two come downward.[33,37] For this reason, the experimental STM only shows one nodal plane since the outermost pyrrole groups are more intense in the STM image for 0.92 V and in agreement with Figure 2c for the LUMO/LUMO+1. The remaining peaks/features at 1.13 and 1.33 V will be discussed in detail later.

Figure 3 shows the density of states as calculated for the molecule in the gas phase, absorbed on Cu_3N−Cu(110) and Cu(110), for Co-d and Co-d_{z^2} states (Figure 3a) and Co-d and Co-π states (Figure 3b). Comparing these results for the C atoms, we observed that peaks are wider for molecules on Cu(110) in comparison with the nitride surface, indicating that for these orbitals the Cu_3N monolayer could be promoting a relative decoupling of the molecule. However, the broadening of the peaks for Co-d spin orbitals, particularly Co-d_{z^2}, indicates a strong hybridization of these orbitals, and the decoupling is not true between the substrate and the Co atom existing in the center of the porphyrin macrocycle. It is important to mention that this interaction does not conspire with the strong interaction between Co and TPP macro-cycle, since d_{z^2} orbitals are originally well localized because of the lack of possible hybridization with neighbor atoms due to the symmetry of the orbital. The calculated LUMO\LUMO+1 peak of the Co−TPP adsorbed on the Cu_3N monolayer is located at ∼0.97 eV, consisting of a red-shift of ∼0.05 eV in comparison to the experimental result shown in Figure 2a, and with the strong component of Co-d states located at ∼0.96 eV. It is important to mention that differences in the energetic positions of the experimental and theoretical data are acceptable considering the limitations of DFT. The LUMO and LUMO+1 peaks in Figure 3 are pretty proximate in energy for the Co−TPP free molecule, with two orthogonal π delocalized molecular orbitals. After the absorption on the surface, the symmetry is broken and an enhancement in the calculated LUMO and LUMO+1 splitting is observed. However, this splitting is not sufficiently high for allowing a direct observation in the experimental dI/dV curves, as shown in Figure 2a.

The calculated DOS for the molecule on the surface is in good agreement with the experimental data. A small broadening is observed for C peaks and a large one is observed for the Co-d orbital. The intensity of the peaks at negative bias voltages is much lower in the experimental case and is most likely due to the following factors. First, the tip/molecule interactions were not included in the simulated DOS. Second, our theoretical dI/dV curve corresponds to the total DOS projected on all the different electronic states, and thus, it may differ from a local DOS (LDOS) projected at a given position in the vacuum region. This last approximation could give better results, particularly for the intensity of the dI/dV signal, making easier the comparison with the experiments. However, it is not the objective of the present work to incorporate a detailed theoretical dI/dV calculation since the structure of the STM tip is not known, and any consideration would be just an approximation. The total DOS help us in the identification of the orbital/atom origin of the experimental dI/dV peaks.

Regarding the experimental results, the molecular orbital shape is confirmed by dI/dV images at selected energies; see Figure 2c. The experimental maps obtained at 1.13 and 1.33 V look similar with contributions from the macrocycle and phenyl groups. Additionally, according to the calculations, the following Co−TPP LUMO+n (for $n > 1$) states appear at 2 V (Figure 3), with no direct evidence of molecular states in the range between 0.92 and 1.50 V. Regarding the molecular topology, both images look similar, but deep observations allow us to make distinctions between them and a characterization in terms of vibronic states. The spatial imaging and spectroscopic mapping of the individual vibronic states and the comparison with DFT calculations enable the assignment of the vibronic progressions. According to the shift in peak energy, of 200 and 400 meV, the spectroscopic sequence could be assigned to phenyl/porphyrin C−C and phenyl/porphyrin C−H vibrational modes, respectively. These values were obtained by means of vibrational calculations on CoTPP free molecule, utilizing DFT at B3LYP/6-31(g) level of theory with Gaussian09.[28] According to this procedure, the Co−TPP vibrational spectrum shows strong electric dipole mediated transitions at 1650 cm^{-1} (203 meV) corresponding to phenyl modes and 3290 cm^{-1} (400 meV) corresponding to C−H modes. The energy of these transitions is very close to the observed peak energy shift of 0.20 and 0.40 eV in reference to LUMO/LUMO+1, giving place to peaks at 1.13 and 1.33 V. It is important to mention that the presented theoretical STM images did not include the vibrational contribution to the theoretical STM images, but this could be the subject of further work. Additionally, we have performed further calculation in order to discard the electronic origin of the vibronic peaks. The simulations checked that the energy splitting of the π-orbitals does not depend on the coordination site of the cobalt atom on the Cu_3N surface, even in the case of interacting with N. When the Co−TPP interacts with a N-vacancy in the Cu_3N monolayer and spin and LUMO/LUMO+1 splittings are observed, the splitting does not exceed ΔE = 165 meV. Because of the value of the charge splitting, the shape of LUMO orbitals, and the corresponding energy splitting for the vibronic modes, we have assumed that the states located at 1.13 and 1.33 V correspond to vibronic states. Finally, the inspection of Figure 2b indicates that the image collected at 1.13 V presents a contribution localized at phenyl and pyrrol rings, where the C−C vibrations are most important. In the case of the image collected at 1.33 V, there exist a contribution more localized at the edges of the molecule and in the phenyl group as well, in concordance with the localization of the C−H bonds. In summary, the mechanism corresponds to an electron from

dx.doi.org/10.1021/jp4013625 | J. Phys. Chem. C 2013, 117, 15984−15990

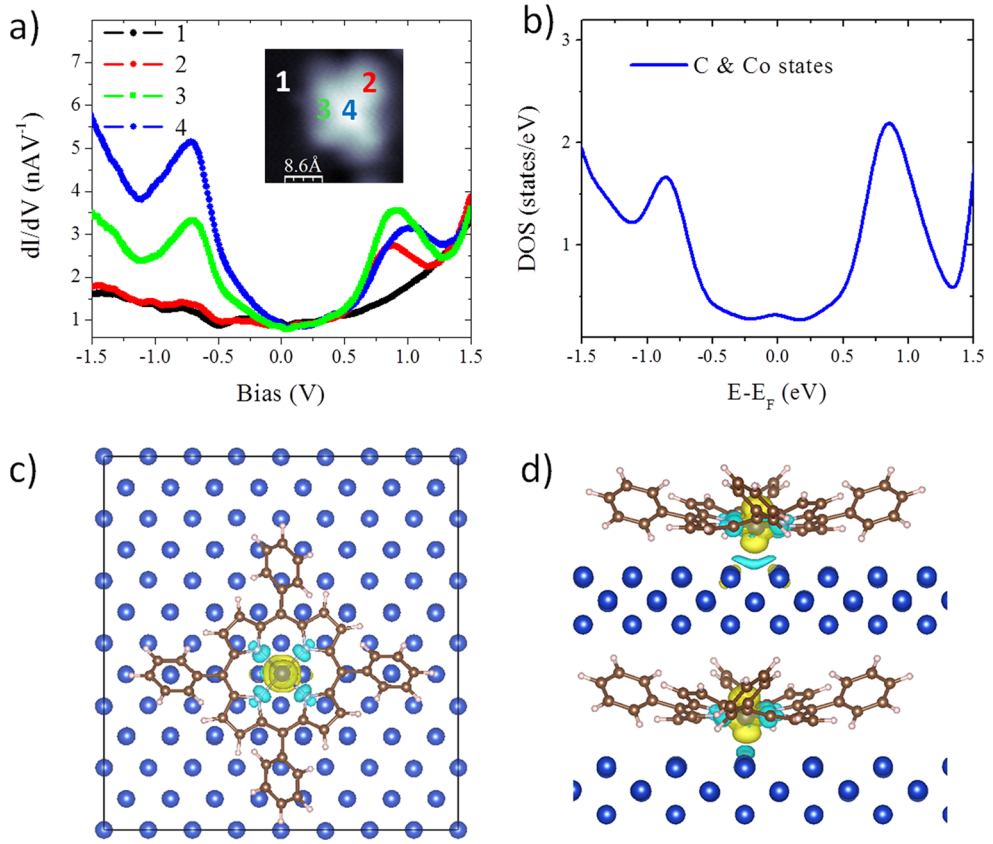

Figure 4. (a) dI/dV spectroscopy taken at different positions on a Co−TPP molecule on Cu(110) and (b) the corresponding theoretical DOS curve from carbon and Co atoms. The inset image was record at 32 mV bias voltage and 1.0 nA tunneling current. Top view (c) and view of the Co−TPP molecule between two[1−10] rows adopting the saddle conformation (d).

the STM tip that tunnels resonantly into a vibronic state of the molecular orbital. Then the electron leaves the molecule tunneling into the substrate, and the molecule returns to its neutral state and stay maybe in a vibrationally excited state.

The localized vibronic modes could be generated nonlocally through the delocalized π-electron state of the TPP skeleton. For this reason, the spatial images for the different vibronic modes present the same spatial distribution of the molecular orbital that contains the modes. Following to the Franck−Condon principle, the vibronic transitions between two LUMO states can be ruled out due to their poor overlap with the substrate, as confirmed by our calculations when the orbitals of the porphyrin core remain almost unmodified, in difference to the states coming from the Co atom in the CoTPP molecule.[38]

Moreover, the simulations for the CoTPP molecule on Cu_3N−Cu(110) show that there exists a very low contribution from Co-d_{z^2} states at the Fermi level. Therefore, the peak, experimentally located at 0 eV cannot be attributed only to the Co−TPP molecule or the Cu_3N substrate because of its unusually high intensity, leaving open the possibility of a Kondo-type contribution.

Co−TPP Molecule on a Clean Cu(110). Figure 4a shows the dI/dV spectra of the Co−TPP molecule on a clean Cu(110) substrate taken at different positions, as indicated in the inset. Image was recorded at 32 mV bias voltage and 1.0 nA tunneling current. The spectrum for the substrate is also presented for comparison (position 1). At the center of the molecule (position 4), two peaks at −0.72 and 1.0 V are observed, and they are attributed to occupied HOMO and unoccupied LUMO/LUMO+1 orbitals, respectively.

When comparing the spectra acquired at different positions on the molecule, a shift is observed of the LUMO/LUMO+1 peak position that is proportional to distance from the Co atom, i.e., 1.0 eV at the center of the molecule (position 4), 0.91 eV at the pyrrolic ring of the porphyrin macrocycle (position 3), and 0.86 eV at the methine bridge of the porphyrin macrocycle, region connected to the phenyl ring (position 2). This behavior is expected and arises from the competition between the contribution of the C levels and the Co-d level to the LDOS. Similar results have been observed for Cu phthalocyanine on NiAl(110).[9] Moreover, the HOMO peak decreases in intensity without any shift in energy when the dI/dV spectra are measured at different positions from the center to the phenyl ring, suggesting that the main contribution to this molecular orbital is from the Co-d spin down orbitals, as shown in Figure 3. For the spectrum obtained on position 2, only the LUMO peak is observed, analogous to H_2−TPP molecules on Ag(111)[39] and on Cu_3Au(100) substrates (result not shown), confirming that at this position the Co atom does not contribute to the tunneling current. This behavior is also supported by the calculations, which show that the distance between the Co and both Cu atoms at the Cu(1$\bar{1}$0) row is approximately d_{Co-Cu} = 2.87 Å (Figure 4b), which is higher than the distance for cobalt to nitrogen of d_{Co-N} = 2.72 Å in Cu_3N−Cu(110) substrates (Figure 1d).

The optimized geometry of the CoTPP molecule corresponds to a saddle conformation according to Donovan et al.[37] Nevertheless, it is important to mention that there are some differences, mostly related to the degree of distortion of the molecule, which is directly linked to the type of xc-potential

dx.doi.org/10.1021/jp4013625 | J. Phys. Chem. C 2013, 117, 15984−15990

used in the DFT calculations. We selected GGA-PBE, and Donovan et al. utilized a postcorrection scheme of the Langreth−Lundqvist van der Waals density functional (vdW-DF); see ref 37.

CONCLUSIONS

The combined DFT study and LT-STM results support the use of the copper nitride as a spacer layer between the tetraphenylporphyrin molecule and the metallic substrate. The combination of the topological corrugation and the chemical nature of the Cu_3N monolayer clearly reduces selectively the hybridization of the C levels of the adsorbed molecule and support a strong hybridization of the Co-d_{z^2} orbital. In this case, the corrugation of the copper nitride behaves as an anchor for the Co−TPP molecule, favoring the interaction between the Co atom in the center of the porphyrin and the higher N atom on the reconstruction, inducing not only chemical but also physical decoupling of the porphyrin macrocycle to the underlying Cu substrate. However, despite the fact that a stronger interaction with the Cu(110) metallic substrate causes an asymmetry in the molecular geometry, a smaller hybridization of Co-d levels is detected when comparing to the Cu_3N layer. This fact is a consequence of the configuration of the Co atom for the single molecular adsorbate, enabling Co-d levels similar to the ones for free molecules.

In summary, experimental and theoretical results support the idea of Cu_3N monolayer as a decoupling layer for tetraphenylporphyrin molecules that possess a central Co atom. The decoupling feature is no longer true for cobalt, which presents a strong interaction with N of the Cu_3N surface. This opens up the possibility to investigate native molecular orbitals and vibronic states of molecules that are not completely electrically isolated from the surface and pinned to a specific site. The reverse behavior was observed for molecular adsorption on a metallic Cu(110) surface. These coupling properties are important to understand the development of future molecular electronic devices. Appropriate matching of molecule architecture and substrate configuration is also an important aspect for future fundamental and applied studies.

AUTHOR INFORMATION

Corresponding Author

*(A.A.P.) Tel: +55-48-32340599. E-mail: andre.pasa@ufsc.br.

Notes

The authors declare no competing financial interest.

ACKNOWLEDGMENTS

We are in debted to Prof. J. Kirschner for helpful discussions and for providing the necessary infrastructure for the development of the experiments. We give thanks to Dr. X.-D. Ma for the assistance by preparing the molecular substrates and to the agencies CAPES, FAPESC, and CNPQ (Brazil), and PEDECIBA, CSIC, and ANII (Uruguay) for additional support to this work.

REFERENCES

(1) Vijayaraghavan, S.; Écija, D.; Auwärter, W.; Joshi, S.; Seufert, K.; Seitsonen, A. P.; Tashiro, K.; Barth, J. V. Selective Supramolecular Fullerene−Porphyrin Interactions and Switching in Surface-Confined C-60-Ce(TPP)(2) Dyads. *Nano Lett.* **2012**, *12*, 4077−4083.

(2) Auwarter, W.; Klappenberger, F.; Weber-Bargioni, A.; Schiffrin, A.; Strunskus, T.; Woll, C.; Pennec, Y.; Riemann, A.; Barth, J. V. Conformational Adaptation and Selective Adatom Capturing of Tetrapyridyl-Porphyrin Molecules on a Copper (111) Surface. *J. Am. Chem. Soc.* **2007**, *129*, 11279−11285.

(3) Ogunrinde, A.; Hipps, K. W.; Scudiero, L. A Scanning Tunneling Microscopy Study of Self-Assembled Nickel(II) Octaethylporphyrin Deposited from Solutions on HOPG. *Langmuir* **2006**, *22*, 5697−5701.

(4) Weber-Bargioni, A.; Auwärter, W.; Klappenberger, F.; Reichert, J.; Lefrançois, S.; Strunskus, T.; Wöll, C.; Schiffrin, A.; Pennec, Y.; Barth, J. V. Visualizing the Frontier Orbitals of a Conformationally Adapted Metalloporphyrin. *ChemPhysChem* **2008**, *9*, 89−94.

(5) Auwarter, W.; Schiffrin, A.; Weber-Bargioni, A.; Pennec, Y.; Riemann, A.; Barth, J. V. Molecular Nanoscience and Engineering on Surfaces. *Int. J. Nanotechnol.* **2008**, *5*, 1171−1193.

(6) Buchner, F.; Seufert, K.; Auwaarter, W.; Heim, D.; Barth, J. V.; Flechtner, K.; Gottfried, J. M.; Steinrück, H. P.; Marbach, H. NO-Induced Reorganization of Porphyrin Arrays. *ACS Nano* **2009**, *3*, 1789−1794.

(7) Liao, M. S.; Scheiner, S. Electronic Structure and Bonding in Metal Porphyrins, Metal = Fe, Co, Ni, Cu, Zn. *J. Phys. Chem.* **2002**, *117*, 205−219.

(8) Weber-Bargioni, A.; Reichert, J.; Seitsonen, A. P.; Auwärter, W.; Schiffrin, A.; Barth, J. V. Interaction of Cerium Atoms with Surface-Anchored Porphyrin Molecules. *J. Phys. Chem. C* **2008**, *112*, 3453−3455.

(9) Qiu, X. H.; Nazin, G. V.; Ho, W. Vibronic States in Single Molecule Electron Transport. *Phys. Rev. Lett.* **2004**, *92*, 206102.

(10) Gao, L.; Ji, W.; Hu, Y. B.; Cheng, Z. H.; Deng, Z. T.; Liu, Q.; Jiang, N.; Lin, X.; Guo, W.; Du, S. X. Site-Specific Kondo Effect at Ambient Temperatures in Iron-Based Molecules. *Phys. Rev. Lett.* **2007**, *99*, 106402.

(11) Lee, H. J.; Ho, W. Vibronic Transitions in Single Metalloporphyrins. *ChemPhysChem* **2005**, *6*, 971−975.

(12) Repp, J.; Meyer, G.; Stojkovic, S. M.; Gourdon, A.; Joachim, C. Molecules on Insulating Films: Scanning-Tunneling Microscopy Imaging of Individual Molecular Orbitals. *Phys. Rev. Lett.* **2005**, *94*, 026803.

(13) Chavy, C.; Joachim, C.; Altibelli, A. Interpretation of STM Images: C-60 on the Gold(110) Surface. *Surf. Chem. Phys. Lett.* **1993**, *214*, 569−575.

(14) Lagoute, J.; Kanisawa, K.; Folsch, S. Manipulation and Adsorption-Site Mapping of Single Pentacene Molecules on Cu(111). *Phys. Rev. B* **2004**, *70*, 245415.

(15) Sautet, P.; Joachim, C. Interpretation of Stm Images: Copper-Phthalocyanine on Copper. *Surf. Sci.* **1992**, *27*, 387−394.

(16) Ogawa, N.; Mikaelian, G.; Ho, W. Spatial Variations in Submolecular Vibronic Spectroscopy on a Thin Insulating Film. *Phys. Rev. Lett.* **2007**, *98*, 166103.

(17) Kohn, W.; Sham, L. J. Self-Consistent Equations Including Exchange and Correlation Effects. *Phys. Rev.* **1965**, *140*, 1133.

(18) Hohenberg, P.; Kohn, W. Inhomogeneous Electron Gas. *Phys. Rev. B* **1964**, *136*, B864.

(19) Giannozzi, P.; Baroni, S.; Bonini, N.; Calandra, M.; Car, R.; Cavazzoni, C.; Ceresoli, D.; Chiarotti, G. L.; Cococcioni, M.; Dabo, I.; et al. Quantum Espresso: A Modular and Open-Source Software Project for Quantum Simulations of Materials. *J. Phys.: Condens. Matter* **2009**, *21*, 395502.

(20) Ma, X.-D.; Bazhanov, D. I.; Fruchart, O.; Yildiz, F.; Yokoyama, T.; Przybylski, M.; Stepanyuk, V. S.; Hergert, W.; Kirschner, J. Strain Relief Guided Growth of Atomic Nanowires in a Cu_3N−Cu(110) Molecular Network. *Phys. Rev. Lett.* **2009**, *102*, 205503.

(21) Kresse, G.; Furthmüller, J. Efficient Iterative Schemes for ab Initio Total-Energy Calculations Using a Plane-Wave Basis Set. *Phys. Rev. B* **1996**, *54*, 11169.

(22) Kresse, G.; Furthmüller, J. Efficiency of ab Initio Total Energy Calculations for Metals and Semiconductors Using a Plane-Wave Basis Set. *Comput. Mater. Sci.* **1996**, *6*, 15.

(23) Kresse, G.; Hafner. Ab Initio Molecular Dynamics for Open-Shell Transition Metals. *Phys. Rev. B* **1993**, *48*, 13115−13118.

(24) Kresse, G.; Hafner, J. Ab Initio Molecular-Dynamics Simulation of the Liquid-Metal-Amorphous-Semiconductor Transition in Germanium. *Phys. Rev. B* **1994**, *49*, 14251.
(25) Perdew, J. P.; Burke, K.; Ernzerhof, M. Generalized Gradient Approximation Made Simple. *Phys. Rev. Lett.* **1996**, *77*, 3865.
(26) Blöchl, P. E. Projector Augmented-Wave Method. *Phys. Rev. B* **1994**, *50*, 17953−17979.
(27) Kresse, G.; Joubert, D. From Ultrasoft Pseudopotentials to the Projector Augmented-Wave Method. *Phys. Rev. B* **1999**, *59*, 1758−1775.
(28) Frisch, M. J.; Trucks, G. W.; Schlegel, H. B.; Scuseria, G. E.; Robb, M. A.; Cheeseman, J. R.; Scalmani, G.; Barone, V.; Mennucci, B.; Petersson, G. A.; et al. *Gaussian 09* revision A.02; Gaussian, Inc.: Wallingford, CT, 2009.
(29) Zhao, A. D.; Qunxiang, L.; Chen, L.; Xiang, H.; Wang, W.; Pan, S.; Wang, B.; Xiao, X.; Yang, J.; Hou, J. G.; et al. Controlling the Kondo Effect of an Adsorbed Magnetic Ion Through its Chemical Bonding. *Science* **2005**, *309*, 1542−1544.
(30) Ternes, M.; Heinrich, A. J.; Schneider, W. D. Spectroscopic Manifestations of the Kondo Effect on Single Adatoms. *J. Phys.: Condens. Matter* **2009**, *21*, 053001.
(31) Venkataramanan, N. S.; Suvitha, A.; Nejo, H.; Mizuseki, H.; Kawazoe, Y. Electronic Structures and Spectra of Symmetric Meso-Substituted Porphyrin: DFT and TDDFT-PCM Investigations. *Int. J. Quantum Chem.* **2011**, *111*, 2340−2351.
(32) Tersoff, J.; Hamann, D. R. Theory and Application for the Scanning Tunneling Microscope. *Phys. Rev. Lett.* **1983**, *50*, 1998−2001.
(33) Buchner, F.; Warnick, K. G.; Wolfle, T.; Gorling, A.; Steinruck, H. P.; Hieringer, W.; Marbach, H. Chemical Fingerprints of Large Organic Molecules in Scanning Tunneling Microscopy: Imaging Absorbate-Substrate Coupling of Metalloporphyrins. *J. Phys. Chem. C* **2009**, *113*, 16450−16457.
(34) Dion, M.; Rydberg, H.; Schroder, E.; Langreth, D. C.; Lundqvist, B. I. Van der Waals Density Functional for General Geometries. *Phys. Rev. Lett.* **2004**, *92*, 246401.
(35) Dion, M.; Rydberg, H.; Schroder, E.; Langreth, D. C.; Lundqvist, B. I. Van der Waals Density Functional for General Geometries (vol 92, art no 246401, 2004). *Phys. Rev. Lett.* **2005**, *95*, 109902.
(36) Thonhauser, T.; Cooper, R. V.; Li, S.; Puzder, A.; Hyldgaard, P.; Langreth, D. C. Van der Waals Density Functional: Self-Consistent Potential and the Nature of the van der Waals Bond. *Phys. Rev. B* **2007**, *76*, 125112.
(37) Donovan, P.; Robin, A.; Dyer, M. S.; Persson, M.; Raval, R. Unexpected Deformations Induced by Surface Interaction and Chiral Self-Assembly of Co^{II}-Tetraphenylporphyrin (Co−TPP) Adsorbed on Cu(110): A Combined STM and Periodic DFT Study. *Chem.—Eur. J.* **2010**, *16*, 11641.
(38) Huan, Q.; Jiang, Y.; Zhang, Y. Y.; Ham, U.; Ho, W. Spatial Imaging of Individual Vibronic States in the Interior of Single Molecules. *J. Chem. Phys.* **2011**, *135*, 014705.
(39) Comanici, K.; Buchner, F.; Flechtner, K.; Lukasczyk, T.; Gottfried, J. M.; Steinruck, H.-P.; Marbach, H. Understanding the Contrast Mechanism in Scanning Tunneling Microscopy (STM) Images of an Intermixed Tetraphenylporphyrin Layer on Ag(111). *Langmuir* **2008**, *24*, 1897−1901.